Load-carrying Behavior of Unstiffened Elements at Elevated Temperatures in Fire

MARKUS KNOBLOCH and MARIO FONTANA
Institute of Structural Engineering
Steel, Timber and Composite Structures
Swiss Federal Institute of Technology ETH Zurich
IBK, HIL D36.2, ETH Hönggerberg
CH-8093 Zurich, Switzerland

ABSTRACT

Unstiffened elements affect markedly the resistance of commonly used open steel sections under fire conditions. The distinct non-linear material behavior of steel at elevated temperatures requires large strains to activate the increase of cross-sectional capacity due to plastification. The yield line theory in conjunction with temperature-dependent second order elastic theory including equivalent geometric imperfections has been used to describe the load-carrying behavior of unstiffened elements in compression and bending at elevated temperatures in fire. Using both theories, the complete load-carrying behavior in the pre- and post-buckling range can be analyzed. In addition, the results obtained from these analytical solutions were compared to numerical results using a geometrical and physical non-linear finite element approach.

KEYWORDS: structural design, steel constructions, fire resistance, local buckling, yield line theory

NOMENCLATURE LISTING

Latin		**Greek**	
b	width of the element	ε	strain
$e_{0,w}$	equivalent geometric imperfection	$\bar{\lambda}_p$	non-dimensional plate slenderness
E_a	modulus of elasticity of steel	μ	Poisson's ratio
f_p	proportional limit of steel	θ_a	steel temperature
f_ε	strain-dependent stress of steel	σ	stress
f_y	yield stress	ψ_ε	strain ratio at the loaded edge of the element
k	buckling factor corresponding to the strain ratio ψ_ε	**subscripts**	
l_{hw}	buckle half-wavelength	$_a$	steel
$M_{pl,\varepsilon}$	plastic resistance to bending moments of the gross section calculated with f_ε	$_{cr}$	critical
$N_{pl,\varepsilon}$	resistance to axial force of the gross section calculated with f_ε	$_p$	proportional limit
t	thickness of the element	$_\varepsilon$	dependency on strain
w_y	deflection of the element	$_\theta$	dependency on temperature

FIRE SAFETY SCIENCE–PROCEEDINGS OF THE EIGHTH INTERNATIONAL SYMPOSIUM, pp. 223-234

INTRODUCTION

Under fire conditions, steel members heat up rapidly and their strength and stiffness decrease. The stress-strain relationship of steel becomes distinctly non-linear, and the assumption of a linear-elastic ideal-plastic material behavior used in ambient temperature design no longer applies. The material behavior at elevated temperatures requires large strains to activate the increase of cross-sectional capacity due to plastification [1]. Open thin-walled sections such as C-, U-, and I-sections consist of stiffened and unstiffened elements. A stiffened element is defined as a flat element, in which both edges parallel to the direction of loading are supported, and an unstiffened element is a flat element, in which only one longitudinal edge is supported. Since unstiffened elements are often used as parts of cross-sections, accurate calculation methods for the resistance of these elements during fires are important. For instance, unstiffened elements used as flanges of I-sections in major and minor axis bending have a strong influence on the bending resistance. The effective width method is commonly used to consider local buckling and to calculate the resistance of unstiffened elements. However, stress-based design methods with effective widths are not suitable to analyze the complete load-carrying behavior including the decreasing branch; which is necessary to determine the resistance of composed sections in fire. Under fire conditions, local buckling needs to be considered for a wider range of plate slenderness than in ambient temperature design [1]. The mechanism of failure of thin-walled steel sections may be analyzed by using yield line theory. In particular unstiffened elements exhibit a local plastic mechanism at collapse. An approach based on yield line theory in conjunction with temperature-dependent second order linear-elastic theory, taking into account initial geometrical imperfections is used in this paper to describe the load-carrying behavior of unstiffened elements at elevated temperatures under fire conditions in the pre- and post-buckling range.

ELASTIC LOAD-DEFLECTION BEHAVIOR

A complex formula to describe the elastic post-buckling behavior of unstiffened elements (steel plates supported on three sides) at ambient temperature was developed by *Kalyanaraman/Peköz* [2]. The analytical solution of square stiffened elements (steel plates supported on all four sides) in compression is much easier. The elastic pre- and post-buckling behavior of stiffened elements with different in-plane boundary conditions may be analyzed using formulae published by *Murray* [3]. For a square steel plate that is simply supported perpendicular to the plane of the plate and free regarding longitudinal and transverse displacements in the plane of the plate (with the additional requirement that the longitudinal edges have to stay straight), a simple relationship between the mean stress $\bar{\sigma}_{x,\theta}$ and the deflection in the middle of the plate $w_{y=b/2}$ is given in Eq. 1 [4]. Based on Eq. 1, a formulation for plates with geometrical imperfections $e_{0,w}$ was developed by *Wittek* [5], given in Eq. 2. The equations can be used at elevated steel temperatures assuming elastic behavior for the solutions. The temperature-dependent critical buckling stress $\sigma_{cr,\theta}$ may be calculated with Eq. 3.

$$\bar{\sigma}_{x,\theta} = \sigma_{cr,\theta} + \frac{\pi^2 \cdot E_{a,\theta}}{8 \cdot b^2} \cdot w_{y=b/2}^2 \qquad (1)$$

$$\bar{\sigma}_{x,\theta} = \left[\sigma_{cr,\theta} + \frac{\pi^2 \cdot E_{a,\theta}}{8 \cdot b^2} \cdot \left(w_{y=b/2}^2 + 3 \cdot w_{y=b/2} \cdot e_{0,w} + 2 \cdot e_{0,w}^2 \right) \right] \cdot \frac{w_{y=b/2}}{w_{y=b/2} + e_{0,w}} \tag{2}$$

$$\sigma_{cr,\theta} = k \cdot \frac{\pi^2 \cdot E_{a,\theta}}{12 \cdot \left(1 - \mu^2\right)} \cdot \left(\frac{t}{b} \right)^2 \tag{3}$$

Figure 1 shows the elastic load-deflection behavior according to Eqs. 1 (Wolmir) and 2 (Wittek). The results are given for ambient temperature and for a steel temperature of 500°C. In addition, geometrical non-linear elastic results calculated with the finite element approach [6] are presented. The numerical results are almost identical with the analytical results. Supplementary, geometrical and physical non-linear numerical calculations with initial imperfections were performed and the results for three non-dimensional plate slenderness ratios calculated at ambient temperature (Eq. 4) are presented as examples.

$$\bar{\lambda}_p = \sqrt{\frac{f_y}{\sigma_{cr}}} \tag{4}$$

The material behavior was assumed to be elastic ideal-plastic for ambient temperature and elastic non-linear plastic for elevated temperatures according to [7]. The load-deflection behavior of stiffened elements with elastic-plastic material behavior at ambient temperature is identical with linear-elastic material behavior, until the ultimate load is almost reached. The load-deflection behavior of the steel plates at elevated temperatures was much softer than at ambient temperature (Fig. 1). The load-deflection curve still increased after the elastic-plastic curve diverged from the linear elastic curve, due to the non-linear plastic material behavior of steel at elevated temperatures. The load-carrying capacity was reached for larger deflections $w_{y=b/2}$ compared to ambient temperature conditions.

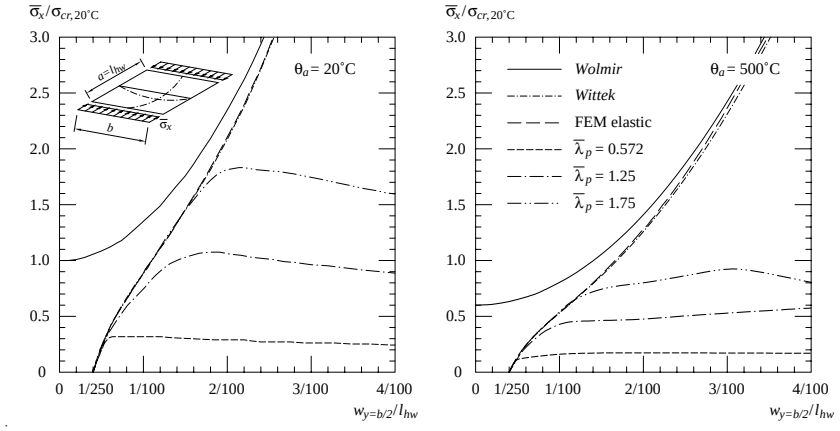

Fig. 1. Load-deflection behavior of a stiffened square element (simply-supported on four sides) at ambient temperature (left) and at a steel temperature of 500°C (right).

UNSTIFFENED COMPRESSION ELEMENTS AT ELEVATED TEMPERATURE

The complete load-deflection behavior of steel columns and plates can be described by using geometrical non-linear elastic theory including equivalent geometric imperfections, as described in the previous section, in combination with plastic theory. The elastic theory is used for the elastic buckling and the second order plastic theory is used for the post-buckling range, necessary to analyze ductility. The load-deflection behavior of an imperfect pin-ended column of compact cross-section (without local buckling) according to second order elastic theory is characterized by an increase of the deflection w with increasing axial force N (Fig. 2 left-dotted line). The load-deflection behavior according to second order rigid-plastic theory (plastic hinge theory) changes in the opposite direction: The resistance N decreases when the deflection w increases. The point of intersection represents an upper bound $N_{u,\max}$ of the actual ultimate load N_u of the column, considering total elastic behavior of the column until the plastic hinge develops. The load-deflection curve of a deformation-controlled experiment (Fig. 2 left-continuous line) of a column with elastic ideal-plastic material behavior follows second order elastic theory at low loads. Due to the plastification of parts of the cross-section, the structure softens and the load-deflection curve falls below the elastic curve. After exceeding the ultimate load N_u, the load-carrying capacity of the column decreases with further increasing deflections w and converges to the load-deflection curve according to second order plastic theory. Differences between the point of intersection $N_{u,\max}$ and the ultimate load N_u result from the assumption of total elastic behavior up to failure. The differences increase with increasing plastic reserves and depend on the cross-section. For instance, the assumption leads to inaccurate results for I-sections in minor axis bending.

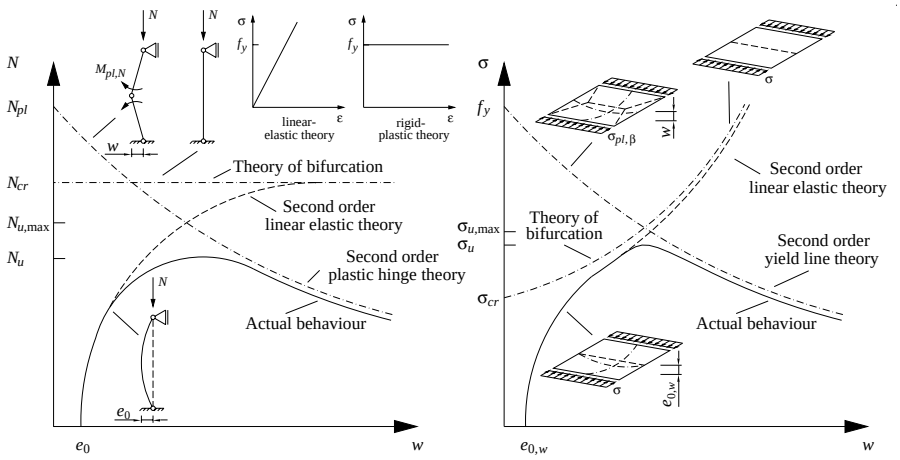

Fig. 2. Load-deflection behavior. Column without local buckling (left); local buckling of a steel plate (right).

The collapse of thin-walled cross-sections, that develop local buckling is characterized by a local plastic mechanism. Local plastic mechanisms may be analyzed using yield lines perpendicular and inclined to the direction of thrust. *Murray* [8] developed an interaction formula (Eq. 5) for an axial force N and a bending moment M for yield lines, rotated by an angle β to the direction of thrust. This formula is based on a simplified stress criterion; the separation of the stress in the inclined yield line into normal stress and shear stress is neglected, but the influence on the results is very small for typical values of β.

$$M_{pl,N,\beta} = M_{pl,N} \cdot \frac{1}{\cos^2 \beta} = M_{pl,N} \cdot \sec^2 \beta = M_{pl} \left[1 - \left(\frac{N}{N_{pl}} \right)^2 \right] \cdot \sec^2 \beta \tag{5}$$

The load-carrying capacity as a function of the deflection was formulated for eight plastic mechanisms by *Murray/Khoo* [9]. Their third mechanism is given in Fig. 3 and may be used to analyze unstiffened elements used as the flanges of I- or U-sections. The plastic mechanism is made of two inclined yield lines and one yield line perpendicular to the direction of thrust. Figure 3 shows a part of the mechanism with the infinitesimal width d*b*. Rotational equilibrium of the element results in:

$$\begin{aligned} dN \cdot w_y &= M_{pl,N} + M_{pl,N,\beta} = M_{pl,N} \cdot \left(1 + \sec^2 \beta\right) = \\ &= M_{pl} \cdot \left[1 - \left(\frac{N}{N_{pl}} \right)^2 \right] \cdot \left(1 + \sec^2 \beta\right) \end{aligned} \tag{6}$$

$$\frac{dN}{dN_{pl}} = \sqrt{\left[\frac{2 w_y}{\left(1 + \sec^2 \beta\right) \cdot t} \right]^2 + 1} - \frac{2 w_y}{\left(1 + \sec^2 \beta\right) \cdot t} \tag{7}$$

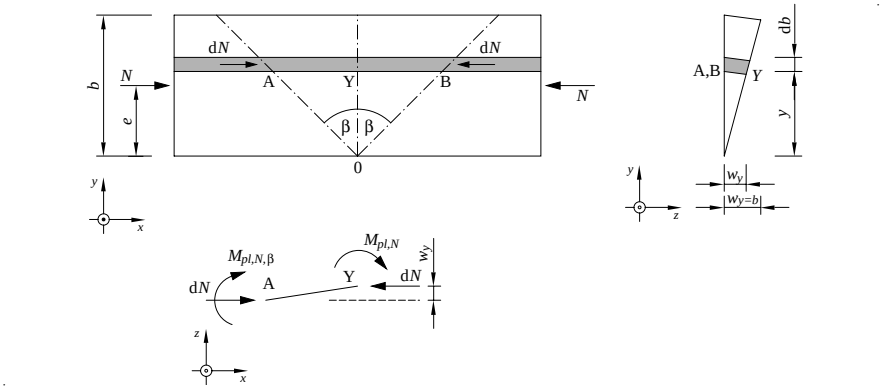

Fig. 3. Local plastic mechanism for unstiffened elements.

The deflection w_y of the element was assumed to be linear over the width *b*, given by Eq. 8.

$$w_y = \frac{y}{b} \cdot w_{y=b} \tag{8}$$

Due to the non-linear material behavior of steel at elevated temperatures under fire conditions, large deflections w_y and corresponding strains ε may result in an increase of the resistance and a plastic zone develops. The results show that the approach using yield lines instead of plastic zones as well as the assumption of linear deflection over the width

(Eq. 8) and the concentration of the curvature of the plate in the yield line was sufficiently precise. The advantage of these assumptions is that the relative load-deflection behavior is independent of temperature.

An angle $\beta = 45°$ between the inclined yield lines and the direction of thrust was observed experimentally at ambient temperature in [10] and is used in this study. Figure 4, e.g., shows the stress distribution for an element with a non-dimensional plate slenderness ratio $\bar{\lambda}_p = 3.0$ at ambient temperature. The relative stress at the non-supported longitudinal edge of the plate decreased if the local buckling deflection $w_{y=b}$ increased. Therefore, the axial load resistance decreased due to the interaction between bending moment M and axial load N of the local plastic mechanism. The local plastic mechanism for unstiffened elements does not allow using simple stress blocks in contrast to the effective width method (see Fig. 4 right). When Eq. 8 is substituted into Eq. 7, which is then integrated, the expression for the relative plastic axial resistance that considers local buckling deflections of an unstiffened element is obtained, Eq. 9. The distribution of the longitudinal stress $\sigma_{x,\theta}$ leads to a bending moment M (formulated in Eq. 10 about an axis normal to the plane of the plate through the longitudinal supported edge).

$$\frac{N}{N_{pl}} = \frac{1}{2} \cdot \left\{ \sqrt{\left[\frac{2 \cdot w_{y=b}}{\left(1+\sec^2\beta\right) \cdot t} \right]^2 + 1} - \frac{2 \cdot w_{y=b}}{\left(1+\sec^2\beta\right) \cdot t} + \frac{\left(1+\sec^2\beta\right) \cdot t}{2 \cdot w_{y=b}} \cdot \ln\left(\sqrt{\left[\frac{2 \cdot w_{y=b}}{\left(1+\sec^2\beta\right) \cdot t} \right]^2 + 1} - \frac{2 \cdot w_{y=b}}{\left(1+\sec^2\beta\right) \cdot t} \right) \right\} \tag{9}$$

$$\frac{M}{M_{pl}} = \frac{t^2 \cdot \left(1+\sec^2\beta\right)}{6 \cdot w_{y=b}^2} \cdot \left(\left\{ \left[\frac{2 \cdot w_{y=b}}{\left(1+\sec^2\beta\right) \cdot t} \right]^2 + 1 \right\}^{\frac{3}{2}} - 1 - \left[\frac{2 \cdot w_{y=b}}{\left(1+\sec^2\beta\right) \cdot t} \right]^3 \right) \tag{10}$$

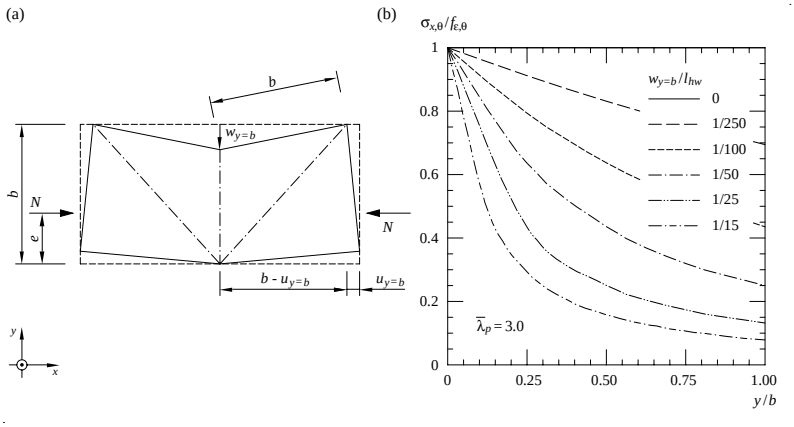

Fig. 4. Local plastic mechanism. (a) Geometrical relationships; (b) Stress distribution.

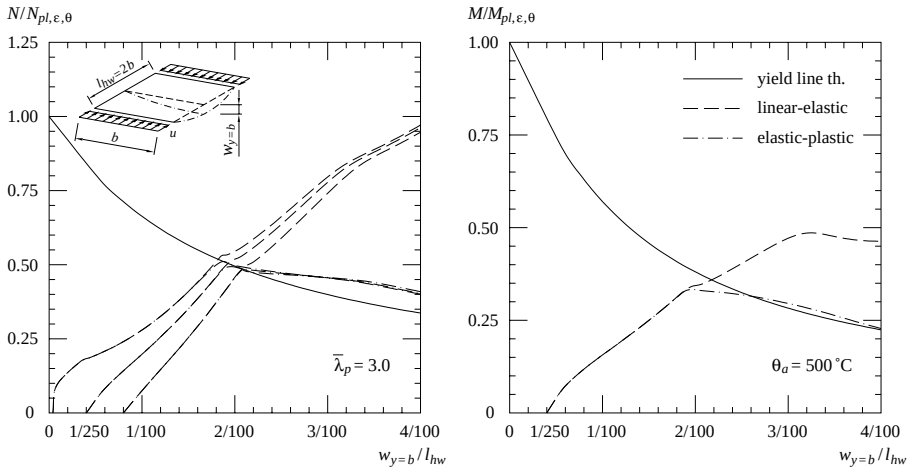

Fig. 5. Load-deflection behavior and corresponding moment-deflection behavior of an unstiffened element in compression ($\psi_\varepsilon = 1.0$) at a steel temperature of 500°C.

Figure 5, e.g., presents the load-deflection curves for a non-dimensional plate slenderness ratio $\bar{\lambda}_p = 3.0$ – considering the buckling coefficient $k = 0.425 + 1/\alpha^2$ – and a steel temperature θ_a of 500°C. In addition to the results according to yield line theory (continuous line) the results according to second order elastic theory considering initial imperfections and according to elastic non-linear plastic theory calculated numerically are shown by dotted lines. The calculations were performed for unstiffened elements in compression ($\psi_\varepsilon = 1.0$). A length-to-width ratio $\alpha = 2$ was chosen. This corresponded to one buckle half-wavelength for the first eigenvalue according to linear elastic theory and a local plastic mechanism whose yield lines are inclined at $\beta = 45°$. The in-plane boundary conditions of the plate were similar to those of calculations for the stiffened element presented in the previous section: the edges remain straight, but were free to displace in-plane. The local plastic mechanism using yield lines had these boundary conditions until the third yield line developed. The third yield line caused a kink at the longitudinally supported edge and the strain ratio changed to $\psi_\varepsilon = 0.0$ after development of the plastic mechanism. A longitudinal displacement u was obtained at the free edge after the development of the three yield lines, while the supported longitudinal edge remained unchanged. In numerical calculations this change was not possible and these differences between the models resulted in slightly different resistances.

The finite element calculations were performed for different values of the initial imperfection $e_{0,w}$, temperatures θ_a between 20° and 1100°C, and temperature-dependent linear-elastic and elastic non-linear plastic material behavior according to [7]. Figure 5 (left) shows the load-deflection behavior of unstiffened elements with initial imperfections of $e_{0,w} = l_{hw}/2500$ and $l_{hw}/125$ in addition to $e_{0,w} = l_{hw}/250$. The value of the initial imperfection had almost no influence on the load-carrying capacity after exceeding the relative maximum. This corresponds to yield line theory, which is independent of initial imperfections. The resistance according to this plastic approach is a function of the deflection $w_{y=b}$ exclusively. Nevertheless, the initial geometrical imperfections influence the elastic load-carrying capacity in the pre- and post-buckling ranges.

In addition to an axial load N a bending moment M about the centre of gravity developed as a result of the non-linear stress distribution of unstiffened elements. Figure 5 (right) shows the relationship between the deflection $w_{y=b}$ and the relative bending moment at the longitudinal edge according to Eq. 10. In order to show local buckling effects, the forces and moments are presented in relation to the strain-dependent plastic resistance. The strain-dependent plastic resistance $f_{\varepsilon,\theta}$ at elevated steel temperatures θ_a is calculated according to [7].

$$N_{pl,\varepsilon,\theta} = \begin{cases} b \cdot t \cdot f_{p,\theta} & if\ \varepsilon \le \varepsilon_{p,\theta} \\ b \cdot t \cdot f_{\varepsilon,\theta} & if\ \varepsilon_{p,\theta} < \varepsilon < \varepsilon_{2.0,\theta} \end{cases} \tag{11}$$

$$M_{pl,\varepsilon,\theta} = \begin{cases} \frac{b^2}{4} \cdot t \cdot f_{p,\theta} & if\ \varepsilon \le \varepsilon_{p,\theta} \\ \frac{b^2}{4} \cdot t \cdot f_{\varepsilon,\theta} & if\ \varepsilon_{p,\theta} < \varepsilon < \varepsilon_{2.0,\theta} \end{cases} \tag{12}$$

It is further possible to formulate the load-carrying capacity with the load-end shortening curve as would be done in deformation-based experiments instead of the load-deflection curve. The relationship between the local buckling deflection $w_{y=b}$ and the longitudinal displacement $u_{y=b}$ at the non-supported edge for the local plastic mechanism of unstiffened elements is shown in Fig. 4 (left) and can be described with Eq. 13. Using the approximation (14) and the formulation for the strains leads to the calculation of the strain ε as a function of the local buckling deflection $w_{y=b}$ with Eq. 15 (cp. [10]).

$$u_{y=b} = \left(1 - \cos\frac{w_{y=b}}{b}\right) \cdot b \tag{13}$$

$$1 - \cos\phi \approx \frac{1}{2}\phi^2 \tag{14}$$

$$\varepsilon_{tot} = \frac{u_{y=b}}{b} = \frac{w_{y=b}^2}{2b^2} \tag{15}$$

$$\frac{N}{N_{pl}} = \frac{1}{2} \cdot \left\{ \begin{array}{l} \sqrt{\left(\frac{2\sqrt{2\varepsilon_{tot}} \cdot b}{3t}\right)^2 + 1} - \frac{2\sqrt{2\varepsilon_{tot}} \cdot b}{3t} + \\ + \frac{3t}{2\sqrt{2\varepsilon_{tot}} \cdot b} \cdot \ln\left[\sqrt{\left(\frac{2\sqrt{2\varepsilon_{tot}} \cdot b}{3t}\right)^2 + 1} + \frac{2\sqrt{2\varepsilon_{tot}} \cdot b}{3t}\right] \end{array} \right\} \tag{16}$$

The relative resistance as a function of the end shortening according to yield line theory (continuous line) as well as the load-shortening curves according to elastic and elastic non-linear plastic theory calculated numerically (dotted lines) are shown in Fig. 6.

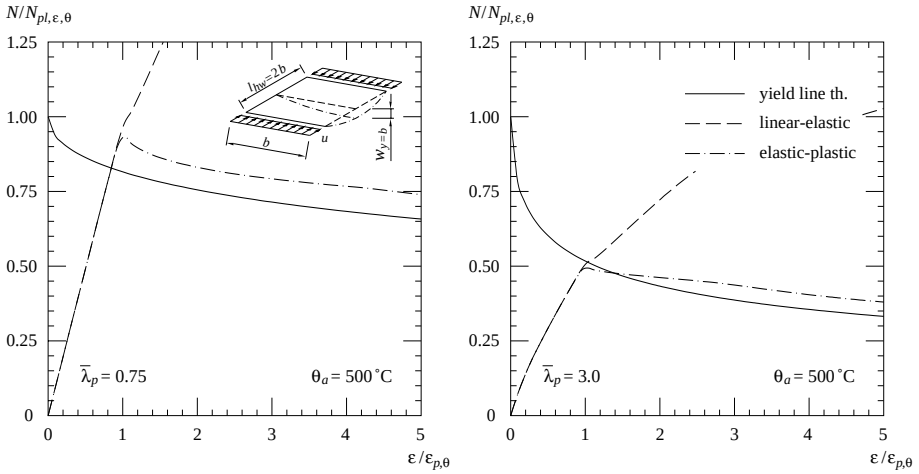

Fig. 6. Load-end shortening behavior of unstiffened elements in compression ($\psi_\varepsilon = 1.0$).

As an example, the results are given for a plate slenderness ratio $\bar{\lambda}_p = 3.0$ (Fig. 6 right). Additionally, the results of a less slender unstiffened element ($\bar{\lambda}_p = 0.75$) are given in Fig. 6 (left). The strain ε is relative to the temperature-dependent strain at the proportional limit $\varepsilon_{p,\theta}$. The relative resistance of the unstiffened element $N/N_{pl,\varepsilon,\theta}$ at the point of intersection between temperature-dependent elastic theory and yield line theory (Fig. 6) was in good agreement (identical) to the relative resistance calculated with the point of intersection of the load-deflection curve (Fig. 5). The point of intersection was approximately at the proportional strain $\varepsilon_{p,\theta}$ as is known from ambient temperature and elastic ideal-plastic material behavior. The relative resistance decreased after exceeding the proportional limit as for ambient temperature, but the absolute value of the resistance could still increase after exceeding the proportional limit due to the non-linear stress-strain relationship [1].

A parametric study for a wide range of plate slenderness ratios confirmed that the point of intersection was almost at the temperature-dependent proportional strain $\varepsilon_{p,\theta}$ for unstiffened elements in compression with non-dimensional plate slenderness ratios $\bar{\lambda}_p > 1.0$. Using yield line theory results in a decrease of the relative resistance with increasing plate slenderness, because the full plastic axial resistance cannot be reached for local buckling deflections $w_{y=b}$ larger than zero, independent of the plate slenderness ratio (Fig. 6 left). The load-end shortening curve according to elastic non-linear plastic theory indicates that the maximum relative resistance of the less slender element is reached at the proportional limit as well.

Starting from the relative load-end shortening behavior given in Fig. 6, a simplified load-end shortening behavior including the ultimate resistance of the unstiffened element can be easily calculated (Fig. 7). Equation 16 is used for the decreasing branch according to yield line theory (Fig. 7 left-continuous lines). The load-carrying behavior for strains

smaller than the temperature-dependent proportional strain is approximated linearly (Fig. 7 left-dotted lines). The whole load-end shortening behavior of unstiffened compression elements (Fig. 7 right) may then be obtained as the product of the relative load-carrying capacity $N/N_{pl,\varepsilon,\theta}$ (linear approximation and Eq. 16) and the strain-dependent ratio of $f_{\varepsilon,\theta}$ to the proportional stress $f_{p,\theta}$ (shown in Fig. 7 left-dotted lines). It can be seen that for low temperatures and high slenderness ratios the load-carrying capacity decreases after exceeding approximately the proportional strain while for high temperatures (between 400°C and 800°C) and low slenderness ratios a further increase is observed.

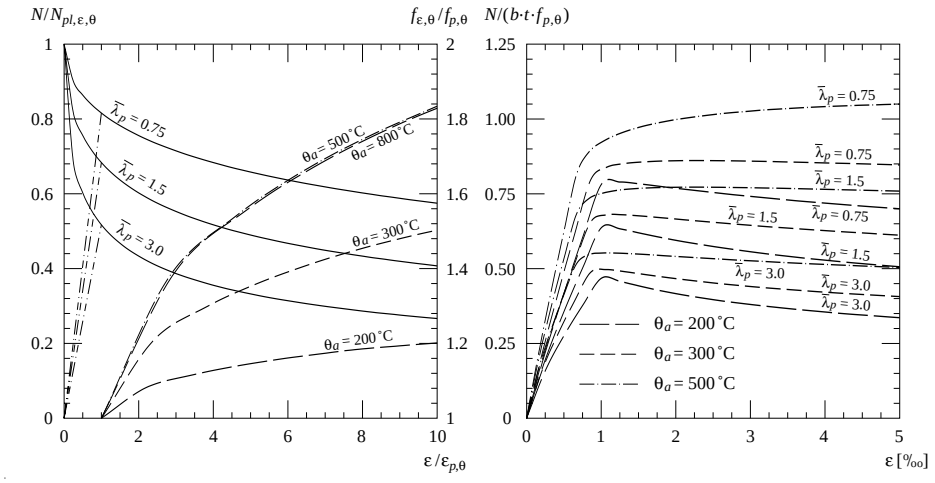

Fig. 7. Calculation of the load-carrying behavior (for steel grade S235).

UNSTIFFENED BENDING ELEMENTS AT ELEVATED TEMPERATURES

The bending resistance of I-sections about the minor axis depends only on the flanges. The maximum strain of these unstiffened elements is located at the non-supported edge and the strain at the supported longitudinal edge (web) is zero. This results in a strain ratio $\psi_\varepsilon = 0.0$. By means of the finite element model described in the previous section, geometrical non-linear numerical calculations of unstiffened elements in bending at ambient and elevated temperatures were performed. As an example, Fig. 8 shows the load-end shortening behavior for two different plate slenderness ratios at a steel temperature of 500°C for elastic and elastic non-linear plastic material behavior according to [7] (dotted lines). In order to verify whether the simplified calculation method presented in the previous section is also suitable for unstiffened bending elements in fire, the results according to the local plastic mechanism developed for uniform compression are also shown (continuous lines). For very large strains the local plastic mechanism may also be used in bending because the stress distribution of a compact I-section (without local buckling) in minor axis bending is assumed to be perfectly plastic (stress blocks). Thus, there is no difference in the assumed stress distribution in compression ($\psi_\varepsilon = 1.0$) and in bending ($\psi_\varepsilon = 0.0$). This behavior of compact sections was applied to slender elements, the stress distribution of slender unstiffened elements being assumed to be independent of the strain distribution as well. For smaller strains large differences exist between the load-end shortening behavior according to yield line theory

(continuous lines) and the actual behavior (dotted lines) calculated numerically. The difference between the upper bound of the relative resistance (obtained as the intersection point between the linear-elastic load-end shortening behavior and the behavior according to yield line theory) and the relative actual resistance calculated with elastic non-linear plastic material behavior results from plastic reserves and increase with increasing reserves, as was described for columns using compact sections in a previous section. In conclusion, temperature-dependent second order elastic theory in conjunction with the local plastic mechanism presented in Fig. 3 is unsuitable for analyzing the load-carrying behavior of unstiffened elements in bending at elevated temperatures. The relative resistance of slender unstiffened elements in bending at elevated temperatures remains constant for large strains (important for cross-sections composed of different stiffened and unstiffened elements) and the load-end shortening behavior according to yield line theory converges to the actual behavior.

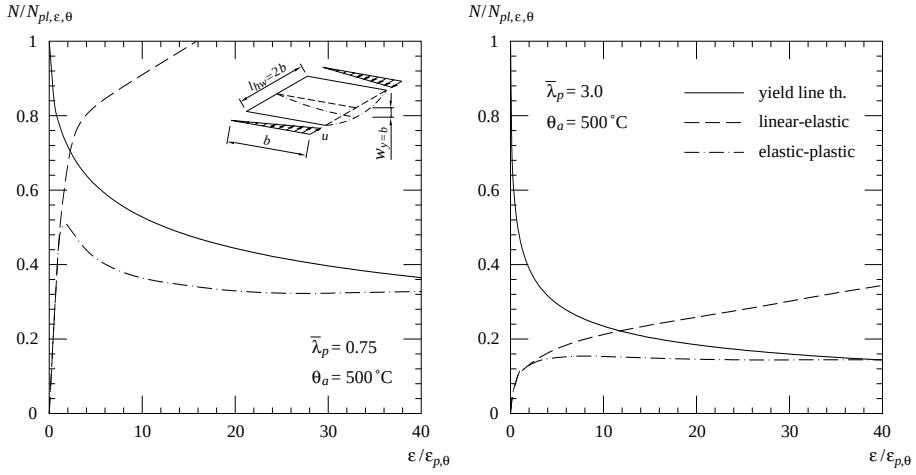

Fig. 8. Load-end shortening behavior of unstiffened elements in bending ($\psi_\varepsilon = 0.0$).

CONCLUSIONS

The load-carrying behavior of unstiffened elements at elevated temperatures under fire conditions has been analyzed using temperature-dependent second order elastic theory considering initial imperfections and yield line theory. Second order elastic theory was used for the pre-buckling range, while a local plastic mechanism with yield lines was used to analyze the decrease of the resistance as a function of the local buckling deflection in the post-buckling range. The relative resistance may be approximated as the point of intersection between both theories. This approximation accords well with results obtained for unstiffened compression elements from numerical calculations using the finite element approach considering temperature-dependent elastic non-linear plastic material behavior. The relative resistance of unstiffened elements in compression at elevated temperatures is almost reached at the temperature-dependent proportional strain, while the relative resistance of unstiffened elements in bending remains constant at large strains. Thus, the absolute resistance of unstiffened compression elements at low temperatures is reached approximately at the proportional limit, while the absolute resistance for unstiffened elements in compression with low slenderness ratios and high

temperatures and of elements in bending increases for strains higher than the proportional strain. This ductile behavior and the non-linear material behavior of steel at elevated temperatures improve the resistance under fire conditions.

The method presented in this paper constitutes the basis for the analysis of steel elements subjected to local buckling and fire. The aim is to develop this method for stiffened elements and also to develop a method for cross-sections composed of stiffened and unstiffened elements and for non-linear temperature distributions so as to take into account both thermal strains and local and global buckling.

REFERENCES

[1] Fontana, M., and Knobloch, M., "Local Buckling Behaviour and Strain-based Effective Widths of Steel Structures Subjected to Fire," *Structures in Fire `04 – Proceedings of the Third International Workshop*, National Research Council Canada, Ottawa, 2004, pp. 71-88.

[2] Kalyanaraman, V., Peköz, T., "Analytical Study of Unstiffened Elements," *Journal of the Structural Division,* **104**, pp. 1507-1524, (1978).

[3] Murray, N.W., *Introduction to the theory of thin-walled structures*, Clarendon Press, Oxford, 1984, pp. 258-268.

[4] Wolmir, A.S., *Biegsame Platten und Schalen*, VEB Verlag für Bauwesen, Berlin, 1962, p. 138.

[5] Wittek, U., *Beitrag zum Tragverhalten der Strukturen bei endlichen Verformungen unter besonderer Beachtung des Nachbeulmechanismus dünner Flächentragwerke*, Institut für Konstruktiven Ingenieurbau, Ruhr-Universität Bochum, Technisch-wisschenschaftliche Mitteilung Nr. 80-1, Bochum, 1980.

[6] Abaqus, *Finite-element Program,* Rel. 6.4.1, Hibitt, Karlson & Sorensen, Inc., 2003.

[7] "Eurocode 3: Design of Steel Structures Part 1.2: Structural Fire Design, Stage 49 Draft," European Committee for Standardisation (CEN), prEN 1993-1.2, Brussels, 2004.

[8] Murray, N.W., "Das aufnehmbare Moment in einem zur Richtung der Normalkraft schräg liegenden plastischen Gelenk," *Die Bautechnik*, **50**, pp. 57-58, (1973).

[9] Murray, N.W., Khoo, P.S., "Some Basic Plastic Mechanisms in the Local Buckling of Thin-Walled Steel Structures," *International Journal of Mechanical Sciences*, **23**, pp. 703-713, (1981).

[10] Rusch, Andreas, *Tragfähigkeit von beulgefährdeten, normalspannungsbeanspruchten I-Profilen*, Shaker, Aachen, 2000.